Journal of Solid State Chemistry **163,** 17–26 (2002)
doi:10.1006/jssc.2001.9333, available online at http://www.idealibrary.com on IDEAL®

A 4D Structural Study of a Ca-Rich Composite-Type Crystal $[A_2Cu_2O_3]_{7+\delta}[CuO_2]_{10}$ with Disorder Phenomena in CuO_2 Sublattice

H. Leligny,*,[1] B. Raveau,* L. I. Leonyuk,† and V. Maltsev†

* *Laboratoire CRISMAT (UMR CNRS), ISMRA, 6 Boulevard du Maréchal Juin, 14050 Caen, France; and* † *Laboratory of Crystal Growth, Chair of Crystallography, Department of Geology, Moscow State University, 119899 Moscow, Russia*
E-mail: henri.leligny@ismra.fr

Received April 9, 2001; in revised from July 17, 2001; accepted August 1, 2001

DEDICATED TO PROFESSOR VON SCHNERING IN HONOR OF HIS 70TH BIRTHDAY

The structure of a Ca-rich composite-type crystal $[A_2Cu_2O_3]_{7+\delta}[CuO_2]_{10}$ with $A = Sr_{0.43}Ca_{0.55}Bi_{0.03}$ and $\delta = 0.04$ was determined by single-crystal X-ray diffraction using the 4D superspace group formalism. Thanks to the existence of a significant number of first-order satellite reflections, reliable results were obtained concerning the displacive modulation within each subsystem. A comparison is made with the accurate structural results obtained by Frost Jensen on similar composite crystals containing less calcium. A larger modulation amplitude is observed in our crystal. Weak interactions (Cu–O ≈ 2.72 Å) are involved locally between the copper atoms of a $[Cu_2O_3]$ layer and one oxygen atom of a $[CuO_2]$ layer, leading in some unit cells to a pyramidal coordination of copper. Such an interaction is not observed in the Ca-less-containing crystal of Frost-Jensen. However, the most important point of this study concerns the evidence for the first time of disorder phenomena inside the $[CuO_2]$ subsystem; this disorder was modeled with both Cu and O splitted sites. Two main configurations with realistic Cu–O bonds are privileged for the CuO_4 squares inside the $[CuO_2]$ sublattice. The refinement results and the bond valence formalism give strong evidence that the *A* sites are occupied at random by Sr and Ca atoms, which display two types of coordination, 7 and 8, in the crystal.

Key Words: **spin ladder cuprates; composite crystal; incommensurate structure; super space group.**

1. INTRODUCTION

Since the discovery of superconductivity at high temperature in copper oxides, a great number of studies has been carried out on the Bi–Sr–Ca–Cu–O system (1). In this system two types of crystals with unusual structural features and fascinating physical properties have been mainly studied. The first type concerns the high-T_C superconducting cuprates $Bi_2Sr_2Ca_{n-1}Cu_nO_{2n+4}$, namely the $n = 1$ and $n = 2$ members called 2201 and 2212, respectively. The complex structure of these superconductors has been studied by many authors (2–6); incommensurate modulations with unusual amplitudes and large local defects are involved, and this modulation arises most probably from the mismatch between two alternate structural slabs of rock salt [BiO, SrO] and perovskite-type $[CuO_2]$ (7). The second type of crystal deals with the spin ladder cuprates $A_{n-1}Cu_{n+1}O_{2n}$ and $[A_2Cu_2O_3]_{m+\delta}[CuO_2]_n$ with A = Ca, Sr, Bi, which have been studied for their spin frustration properties and might be susceptible to exhibiting superconductivity (8–13). The oxides $[A_2Cu_2O_3]_{m+\delta}[CuO_2]_n$ exhibit a composite structure built up from two interpenetrating sublattices with either commensurate or incommensurate periodicities along a single main crystallographic direction, depending on their chemical composition, i.e., on the n/m values. The values most currently observed are rational and very close to each other, i.e., 7/5, 10/7, and 13/9. The deviation from those values, defined by the δ parameter, leads to incommensurate values for the two distinct sublattice parameters and then to an incommensurate structure for the composite crystal. Usually a modulation is involved within each sublattice arising from the mutual influence of the two composite parts and appears as being mainly required to obtain a satisfactory bonding scheme between A cations and oxygen atoms belonging to the $[CuO_2]$ subsystem.

The structure of such composite crystals with an $n/m = 7/5$ or $10/7$ ratio is the most known. Accurate structure determinations were carried out by Frost-Jensen *et al.* (14, 15) on two different orthorhombic crystals denoted I and II. In the first crystal, the $[CuO_2]$ composite part exhibits an F lattice while in the second one a lowering of the translational symmetry (A lattice) is observed at the level of this $[CuO_2]$ sublattice. These authors pointed out that the use of a sufficient number of satellite reflections,

[1] To whom correspondence should be addressed.

0022-4596/02 $35.00

originating from the mutual influence of the two subsystems, is, at least in this type of composite crystal, essential for obtaining reliable results concerning the atomic modulation amplitudes and then a realistic bonding scheme.

The possible existence of disorder phenomena in the $[CuO_2]$ sublattice, as suggested by Wu *et al.* (16), which was not accounted for in the previous works, incited us to revisit the structure of these composite crystals. In this paper, we report on the structural study of a crystal having a larger Ca content ($A = Sr_{0.43}Ca_{0.55}Bi_{0.03}$) than the crystal (I) used by Frost-Jensen ($A = Sr_{0.46}Ca_{0.48}Bi_{0.06}$). As shown from Weissenberg diagrams, the crystalline quality (sharp diffraction spots) of our sample is proved. Otherwise, a set of conspicuous satellite reflections is observed on X-ray oscillating crystal patterns while, usually for spin ladder cuprate crystals, a limited number of satellite reflections is observed using a conventional X-ray source.

2. EXPERIMENTAL

2.1. Synthesis

The crystals studied were grown in air by cooling the melt of composition $2Bi_2O_3$–3SrO–3CaO–6CuO in an alumina crucible. The initial load of the mixture of oxides was heated up to 860°C at a rate 4°h, cooled down to 795°C at the same rate and then quenched. The ladder-phase crystals were extracted mechanically from the voids formed in a partially melted load. According to the X-ray powder diffraction data, the ladder phase was identified as $A_{10}Cu_{17}O_{29}$ (PDF DATA BASE 79-0109). The phases 2201 (PDF 78-2019) and 2212 (PDF 82-2278) were indicated as cocrystallizing phases.

2.2. X-ray Diffraction

The energy dispersive spectroscopy (EDS) analysis of the crystal used for the data collection led to the atomic percentage of 61.9(3), 21.1(3), 16.1(2), 0.9(1) for Cu, Ca, Sr, and Bi, respectively.

Weissenberg photographs were used to check the crystal quality of the sample. X-ray data collection of the reflection intensities was carried out with graphite-monochromatized Mo$K\alpha$ radiation ($\lambda = 0.71073$ Å) on an Enraf–Nonius CAD-4 diffractometer. The cell parameters of the two subsystems were refined independently from standard techniques. Before performing the data collection, several reciprocal [001]* rows were scanned to appreciate the intensity of the satellite reflections and determine their possible orders.

The intensities of the two subsystems of main reflections (orthorhombic symmetry) were registered separately (a quarter of space). The intensities of the satellite reflections of first and second orders were collected afterward, increasing the exposure time up to 120 s for the weakest reflections.

No significant intensity variation higher than 2% was observed during the experiment, for the three standard reflections chosen for each subsystem. Corrections for Lorentz polarization effects and absorption, based on crystal morphology and using a Gaussian integration method, were applied to the data sets with the JANA 98 program (17). Crystal data and experimental results are given in Table 1.

As verified with a squid magnetometer device, the crystal used for the data collection is not superconducting up to 4K under atmospheric pressure.

3. SYMMETRY

The cell parameters of the subsystem v are denoted a_v, b_v, c_v, $v = 1$, refering to the $[A_2Cu_2O_3]$ subsystem, which exhibits reflections of largest intensity. Each composite part has an F orthorhombic lattice with $a_1 = a_2$, $b_1 = b_2$; the $\gamma = c_1/c_2$ ratio (Table 1) deviates from the 7/5 and 10/7 rational values. No obvious correlation between the γ values and the chemical composition is observed for this type of misfit crystals. Otherwise, the action of bismuth on the commensurate or incommensurate character of the modulation is still not well understood in so far as this atom is introduced in very small amounts with Sr and Ca cations. However, for crystals with Ca or Sr extreme composition (15, 18) γ appears as very close to the 10/7 rational value while for the intermediate compositions γ appears as irrational ($\gamma = 1.420$). Since the main reflections of the second subsystem are to be considered as satellite reflections of Mth order of the $hk0$ reflections belonging to the first subsystem (19), if the latter is chosen as reference, the diffraction vector can be then written as $\mathbf{s}^* = h\mathbf{a}_1^* + k\mathbf{b}_1^* + l\mathbf{c}_1^* + M\mathbf{q}_1^*$ with $\mathbf{q}_1^* = \mathbf{c}_2^* + \mathbf{a}_2^* + \mathbf{b}_2^*$. It turns out that $\mathbf{s}^* = H\mathbf{a}_1^* + K\mathbf{b}_1^* + L\mathbf{c}_1^* + M\mathbf{c}_2^*$, where $H = h + M$, $K = k + M$, $L = l$; $\mathbf{c}_2^*$ stands for the irrational part $\mathbf{q}_1^{*ir}$ of $\mathbf{q}_1^*$ with $\mathbf{q}_1^{*ir} = \gamma\mathbf{c}_1^*$.

The condition on hkl leads to the Bravais condition $HKLM$: $H + K = 2n$, $H + L + M = 2n$ and $K + L + M = 2n$, implying the centering $(\frac{1}{2}\,\frac{1}{2}\,0\,0)$, $(\frac{1}{2}\,0\,\frac{1}{2}\,\frac{1}{2})$, and $(0\,\frac{1}{2}\,\frac{1}{2}\,\frac{1}{2})$ in 4D space.

The $HKLO$ and $HKOM$ reflections are then, within this description, the main reflections of the first and second subsystems, respectively, while the others denoted $HKLM$ are the satellite reflections due to the mutual influence of the two composite parts.

Regardless of possible conditions on $H0LM$ and $0KLM$ reflections, several super space groups, namely $Fmmm(00\gamma)ss0$, $Fmm2(00\gamma)ss0$, $Fm2m(00\gamma)s00$, $F2mm(00\gamma)0s0$, and $F222(00\gamma)$ may a priori describe the symmetry of these crystals. Indeed, all these groups allow a right relative ordering of the two component structures $[A_2Cu_2O_3]$ and $[CuO_2]$ both along [100] and [010]. Actually, some $H0LM$ and $0KLM$ satellite reflections with weak intensities and

TABLE 1
Experimental Data

Chemical formula	$[A_2Cu_2O_3]_1[CuO_2]_{1.4200(4)}$	
	$A = Sr_{0.428(2)}Ca_{0.546(2)}Bi_{0.026(3)}$	
Crystal size	$0.74 \times 0.15 \times 0.07\ mm^3$	
Crystal shape	(010) (100) (1$\bar{1}$0) (1$\bar{2}$0) ($\bar{1}$2$\bar{0}$) ($\bar{1}\bar{1}$0) ($\bar{2}$10) (001) (00$\bar{1}$)	
Cell parameters (Å) ($T = 294$ K)		
First subsystem	$a_1 = 11.351(1)$, $b_1 = 12.828(1)$, $c_1 = 3.9088(3)$	
Second subsystem	$a_2 = 11.350(1)$, $b_2 = 12.828(1)$, $c_2 = 2.7528(6)$	
Modulation vector $\mathbf{q}_1^{*ir}$	1.4200(4) $\mathbf{c}_1^*$	
Super space groups		F222(11γ) F222(11γ^{-1})
Z	4	
ρ (g/cm^3), μ (cm^{-1})	5.13	232
Wavelength (Å)	0.71073	
θ_{max}, $(\sin\theta/\lambda)_{max}$	45°, 0.995	
Scan mode	Ω, θ	

Reflection groups	Registered space	Number of measured reflections
Main reflections		
$HKLO$	$-22 \le H \le 22$	1879
	$0 \le K \le 25$	
	$0 \le L \le 7$	
$HKOM$	$-22 \le H \le 22$	959
	$0 \le K \le 25$	
	$0 \le L \le 5$	
Satellite reflections		
$HKML$	$0 \le H \le 18$	1805
	$0 \le K \le 20$	
$L \ne 0$	$-2 \le L \le 9$	
$M \ne 0$	$-2 \le M \le 2$	

Internal consistency factor R_{int} (after absorption corrections)

Subsystem1	(HKLO reflections)	0.043
Subsystem 2	(HKOM reflections)	0.047

Extreme transmission factors

Subsystem 1	0.084	0.282
Subsystem 2	0.087	0.282

Number of unique reflections with $I \ge 3\sigma(I)$

Reflection groups		R and wR reliability factors	
The whole reflections	1015	0·0335	0.0187
$HKLO$	410	0·02590	0.0201
$HKOM$	262	0·0313	0.0206
$HKOO$	100	0.0183	0.0120
$HKL \pm 1$	206	0·0652	0.0541
$HKL \pm 2$	37	0.1290	0.1185

Number of observations/number of refined parameters	13.3
Weighting scheme	$1/\sigma_F^2$
G.o.F	1.8
$\Delta\rho_{min}$ (e/Å^3)	−1.6
$\Delta\rho_{max}$(e/Å^3)	1.7

$I > 3\sigma(I)$ do not follow the conditions $H0LM$, $M = 2n$ and $0KLM$, $M = 2n$ characteristic of the two groups $Fmmm(00\gamma)ss0$ and $Fmm2(00\gamma)ss0$.

4. REFINEMENT

The average coordinates and Fourier terms describing the modulation were refined from the F values with the JANA 98 program (17) starting from the parameter values determined by Frost-Jensen *et al.* (14) (crystal I).

The components of the displacement vector $\mathbf{U}_v^\mu$ of the μth atom in the subsystem v were written as Fourier series limited to the first and second harmonics since the satellite reflections $HKLM$ with $|M| > 2$ were not observed:

$$U_{v,i}^{\mu}(\bar{x}_{4,v}^{\mu}) = \sum_{n=1}^{2} A_{v,i,n}^{\mu} \sin 2\pi n\, \bar{x}_{4,v}^{\mu} + B_{v,i,n}^{\mu} \cos 2\pi n\, \bar{x}_{4,v}^{\mu}.$$

$$v = 1, 2;\ i = 1, 2, 3.$$

$\bar{x}_{4,v}^{\mu} = \mathbf{q}_v^{*ir} \cdot (\mathbf{r}_{0,v}^{\mu} + \mathbf{p}_v) = \mathbf{q}_v^{*ir} \cdot \mathbf{r}_{0,v}^{\mu} + t_v$, where $\mathbf{r}_{0,v}^{\mu}$ and $\mathbf{p}_v$ are the average position of the atom μ in the origin unit cell and a lattice vector of the subsystem v, respectively; as the c_1/c_2 ratio is irrational (incommensurate case), all the t_v values in the [0–1] interval are physical points.

The symmetry of the composite crystal was carefully scrutinized by refining the average atomic positions and the displacive modulation parameters within each of the possible super space groups. Indeed, the observed reflections $H0L \pm 1$ and $0KL \pm 1$ were regarded as not sufficiently numerous to deduce for certain the $F222(00\gamma)$ super space group. The obtained results allowed some points to be specified:

(i) The symmetry $Fmmm(00\gamma)ss0$ can be discarded, the agreement R and wR factors being significantly larger than in the other models.

(ii) The lower symmetries including the m mirrors do not lead to significant improvement of R and wR factors in comparison with the $F222(00\gamma)$ symmetry despite a larger number of parameters to be refined. Otherwise, the modulation of anisotropic displacement parameters (ADPs) (20), considered for A and Cu(1), gives rise to some abnormal high Fourier terms, while within the $F222(00\gamma)$ symmetry the modulation of the ADP is smooth as expected.

(iii) Within all super space groups, anomalies are evidenced at the level of the $[CuO_2]$ subsystem; abnormally large values are observed for ADP-of copper and oxygen atoms, suggesting most probably disorder phenomena within this composite part.

The $F222(00\gamma)$ super space group can be then considered as describing well the actual symmetry of our crystal in agreement with the results established by Frost-Jensen *et al.* on crystal I, collecting satellite reflections from X-ray synchroton radiation. Within this symmetry two models were considered: to set comparisons with the model of Frost-Jensen *et al.*, a first model was refined, assuming single sites for copper and oxygen atoms. A second model, considering a disorder of positional type, was attempted, introducing split sites for both Cu and O atoms; this

TABLE 2
Parameters of the Composite Crystal (in Bold) and Comparison with the Results of Frost–Jensen *et al.* (14)

		First composite part				
		r_0	A_1	B_1	A_2	B_2
A	U_1	$\frac{1}{2}$	− 0.00403(5)	0	− 0.0008(3)	0
		$\frac{1}{2}$	**− 0.00429(5)**	**0**	**− 0.0013(2)**	**0**
	U_2	0.38015(6)	0	0.0006(1)	0	≈ 0
		0.38055(2)	**0**	**0.0005(2)**	**0**	**0.0003(1)**
	U_3	$\frac{3}{4}$	− 0.0003(4)	0	0.0076(2)	0
		$\frac{3}{4}$	**0.0066(4)**	**0**	**0.0088(2)**	**0**
Cu(1)	U_1	0.33421(6)	0	0.003(2)	0	0.0004(1)
		0.33411(2)	**0**	**−0.0004(1)**	**0**	**0.0005(1)**
	U_2	$\frac{1}{4}$	− 0.00421(5)	0	≈ 0	0
		$\frac{1}{4}$	**− 0.00445(5)**	**0**	**≈ 0**	**0**
	U_3	$\frac{1}{4}$	0.0022(4)	0	− 0.0010(2)	0
		$\frac{1}{4}$	**≈ 0**	**0**	**− 0.0011(1)**	**0**
O(1)	U_1	0.1686(4)	0	0·001(1)	0	0.0007(6)
		0.1675(1)	**0**	**0.0020(6)**	**0**	**≈ 0**
	U_2	$\frac{1}{4}$	− 0.0056(3)	0	− 0.002(1)	0
		$\frac{1}{4}$	**− 0.0060(1)**	**0**	**0.006(1)**	**0**
	U_3	$\frac{1}{4}$	− 0.005(2)	0	≈ 0	0
		$\frac{1}{4}$	**≈ 0**	**0**	**≈ 0**	**0**
O(2)	U_1	$\frac{1}{2}$	0	0	0	0
		$\frac{1}{2}$	**0**	**0**	**0**	**0**
	U_2	$\frac{1}{4}$	0	0	0	0
		$\frac{1}{4}$	**0**	**0**	**0**	**0**
	U_3	$\frac{1}{4}$	− 0.009(3)	0	− 0.003(2)	0
		$\frac{1}{4}$	**− 0.020(2)**	**0**	**− 0.003(1)**	**0**
		α_0^{ij}	α_1^{ij}	β_1^{ij}	α_2^{ij}	β_2^{ij}
A	U^{11}	0.0111(1)	0	0.0048(6)	0	≈ 0
	U^{22}	0.0122(1)	0	≈ 0	0	− 0.0013(4)
	U^{33}	0.0109(2)	0	− 0.0025(7)	0	0.0016(2)
	U^{12}	0	− 0.0006(1)	0	− 0.0073(7)	0
	U^{13}	0.0027(2)	0	− 0.0030(2)	0	0.0023(8)
	U^{23}	0	≈ 0	0	≈ 0	0
Cu(1)	U^{11}	0.0050(1)	0	≈ 0	0	≈ 0
	U^{22}	0.0221(2)	0	≈ 0	0	− 0.00021(6)
	U^{33}	0.0037(1)	0	≈ 0	0	− 0.0009(2)
	U^{12}	0	− 0.0006(1)	0	≈ 0	0
	U^{13}	0	− 0.0013(4)	0	≈ 0	0
	U^{23}	0.0048(6)	0	≈ 0	0	− 0.0056(8)
O(1)	U^{11}	0.0063(6)				
	U^{22}	0.023(2)				
	U^{33}	0.0049(7)				
	U^{12}	0				
	U^{13}	0				
	U^{23}	− 0.005(3)				
O(2)	U^{11}	0.0042(7)				
	U^{22}	0.030(1)				
	U^{33}	0.010(1)				
	U^{12}	0				
	U^{13}	0				
	U^{23}	0				

TABLE 2—*Continued*

		Second composite part				
		r_0	A_1	B_1	A_2	B_2
			(a) No split sites			
Cu(2)	U_1	$\frac{1}{4}$	0	0	0	0
		$\frac{1}{4}$	**0**	**0**	**0**	**0**
	U_2	$\frac{1}{2}$	0	0	0	0
		$\frac{1}{2}$	**0**	**0**	**0**	**0**
	U_3	$\frac{1}{4}$	0.010(1)	0	− 0.0086(5)	0
		$\frac{1}{4}$	**≈ 0**	**0**	**−0.0078(3)**	**0**
O(3)	U_1	0.1367(3)	0	≈ 0	0	0.0031(3)
		0.1349(1)	**0**	≈ 0	0	**0.0028(2)**
	U_2	$\frac{1}{2}$	0.0240(5)	0	0.0029(8)	0
		$\frac{1}{2}$	**0.0224(2)**	**0**	**−0.0025(8)**	**0**
	U_3	$\frac{3}{4}$	− 0.009(5)	0	− 0.025(2)	0
		$\frac{3}{4}$	− **0.050(2)**	**0**	**−0.013(1)**	**0**
			(b) split model			
Cu(2)	U_1	$\frac{1}{4}$	0	0	0	0
	U_2	$\frac{1}{2}$	0	0	0	0
	U_3	0.2861(3)	− 0.0020(9)	≈ 0	− 0.0075(3)	≈ 0
O(3)	U_1	0.1347(1)	− 0.0031(5)	≈ 0	0.0039(5)	0.0033(2)
	U_2	0.4944(3)	0.0246(2)	− 0.0075(4)	≈ 0	0.0060(5)
	U_3	0.710(2)	− 0.045(2)	≈ 0	− 0.013(1)	≈ 0

	(a) no split sites	
Cu(2)	U^{11}	0.0076(1)
	U^{22}	0.0172(1)
	U^{33}	0.0308(2)
	U^{12}	0
	U^{13}	0
	U^{23}	0
O(3)	U^{11}	0.0102(4)
	U^{22}	0.032(1)
	U^{33}	0.025(1)
	U^{12}	0
	U^{13}	0
	U^{23}	0.019(2)
	(b) split model	
Cu(2)	U^{11}	0.0076(1)
	U^{22}	0.0173(1)
	U^{33}	0.0210(2)
	U^{12}	≈ 0
	U^{13}	0
	U^{23}	0
O(3)	U^{11}	0.0084(4)
	U^{22}	0.011(1)
	U^{33}	0.017(1)
	U^{12}	0.003(1)
	U^{13}	0.004(1)
	U^{23}	− 0.008(2)

Note. Uncertainties are given in parentheses. The average coordinates are shown in the third column under the symbol r_0. The Fourier coefficients describing the displacive modulation of each subsystem are denoted A_1, B_1, A_2, and B_2, A and B are the sine and cosine terms, respectively, and the 1 and 2 indexes stand for the first and second harmonic respectively. The ADP terms U^{ij} (Å^2) are given in the second part of the table for each subsystem: the α_0^{ij} terms are the average values of U^{ij} while the α^{ij} and β^{ij} terms are the sine and cosine Fourier coefficients of the ADP modulation. The expression used for the Debye–Waller factor is $\exp(-2\pi^2 \sum_{i=1}^{3} \sum_{j=1}^{3} U^{ij} a^{*i} a^{*j} h_i h_j)$.

model improved in a sensible way the reliability R_1 and R_2 factors related to the satellite reflections of first and second order, respectively (0.065 and 0.13 versus 0.072 and 0.16).

Finally the Bi atomic fraction was constrained during the refinement to the value derived from the EDS analysis; only the Ca and Sr fractions were allowed to be refined.

The refined parameters are listed in Table 2. The reliability R_1 and R_2 factors are higher than the R_0 factors obtained for the $HKL0$ and $HK0M$ main reflections (Table 1). This result is to relate mainly to the weak intensity of the whole satellite reflections registered using a conventional X-ray source; a similar R statistic was indeed observed for the weak reflections belonging to the main reflections.

5. DISCUSSION

5.1. Structure Comments

The structure of this composite crystal can be described as the stacking along the [010] direction of $[Cu_2O_3]$ and $[CuO_2]$ layers interleaved with A layers (A = Ca, Sr, Bi) according to the sequence "A, Cu_2O_3, A, CuO_2" with a spacing about 1.6 Å (b/8) (Fig. 1). One CuO_2 layer consists of 1D patterns of edge-sharing CuO_4 squares forming chains along the [001] incommensurate direction (Fig. 2). Inside a Cu_2O_3 layer a 2D network of CuO_4 squares, forming interconnected ribbons in the [001] direction, is observed (Fig. 2); the so-called ladder-structure expression is related to this connection mode between neighboring ribbons, each ribbon built up from edge-sharing CuO_4 squares running in a zig-zag fashion along [001].

The Ca and Sr cationic composition on the A sites deduced from refinements (Table 1) is consistent with the EDS analysis and shows that the studied crystal contains a Ca amount larger than that of the crystal I used by Frost-Jensen *et al.* The Ca concentration in the crystal is expected to influence both the lattice parameters and the modulation behavior. Indeed, first the b_1 cell parameter of our crystal (b_1 = 12.828(1) Å) is smaller than the b_1 cell parameter of the crystal I studied by Frost-Jensen *et al.* (b_1 = 12.960(4) Å). This result, related to the average radius of the A site cations, which decreases as the Ca content increases, is consistent with the study of Pachot (21), who reports the variations of the cell parameters of these spin-ladder crystals versus the Ca content; no change of the other cell parameters is observed, probably because the Cu_2O_3 layers are rigid 2D networks. Second, some Fourier terms describing the modulation are different within the two studies (see Table 2 for a comparison). Two Fourier terms (underlined in Table 2) are significantly larger than those refined by Frost-Jensen *et al.* One is related to the A cation located in the first composite part, while the other concerns the O(3) atom in the second composite part (first model with single Cu(2) and O(3) sites). Note that the other Fourier terms are quite similar in the two studies. These results mean a more marked modulation in the Ca-richer composite crystals, assuming that a sufficient number of satellite reflections is included in our data.

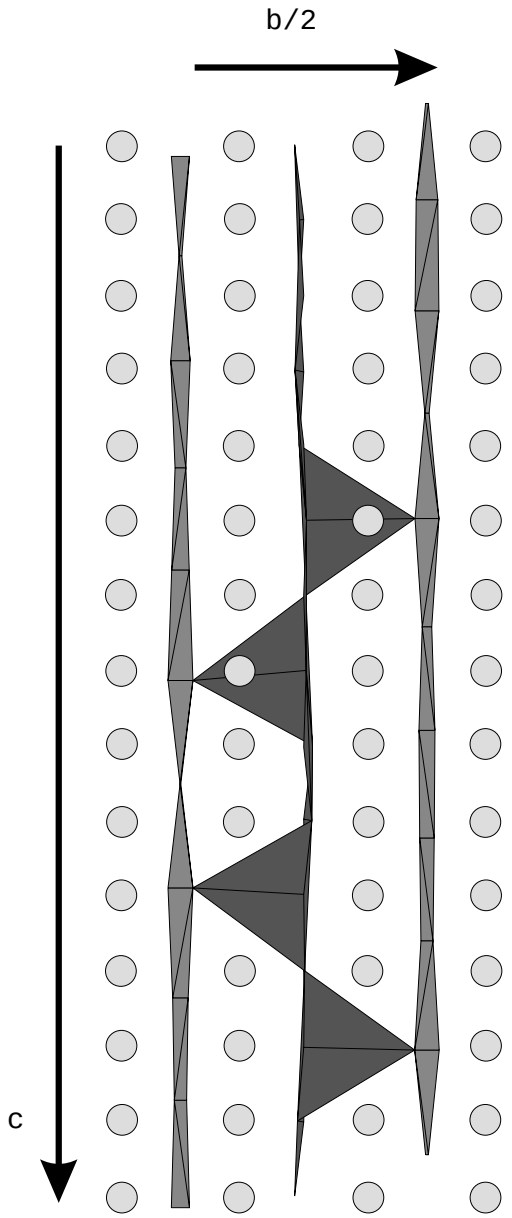

FIG. 1. The alternation along [010] of the $[Cu_2O_3]$, A and $[CuO_2]$ layers. The gray circles denote the A cations. The projection is drawn within the commensurate approximation ($c = 7c_1$), considering for simplicity no split sites in the $[CuO_2]$ sublattice but taking the modulation into account. Note the significant distortion of the CuO_4 square units. Some Cu(1) atoms of the $[Cu_2O_3]$ sublattice would exhibit a 4+1 pyramidal coordination (dark triangles) with apical distances of about 2.7 Å.

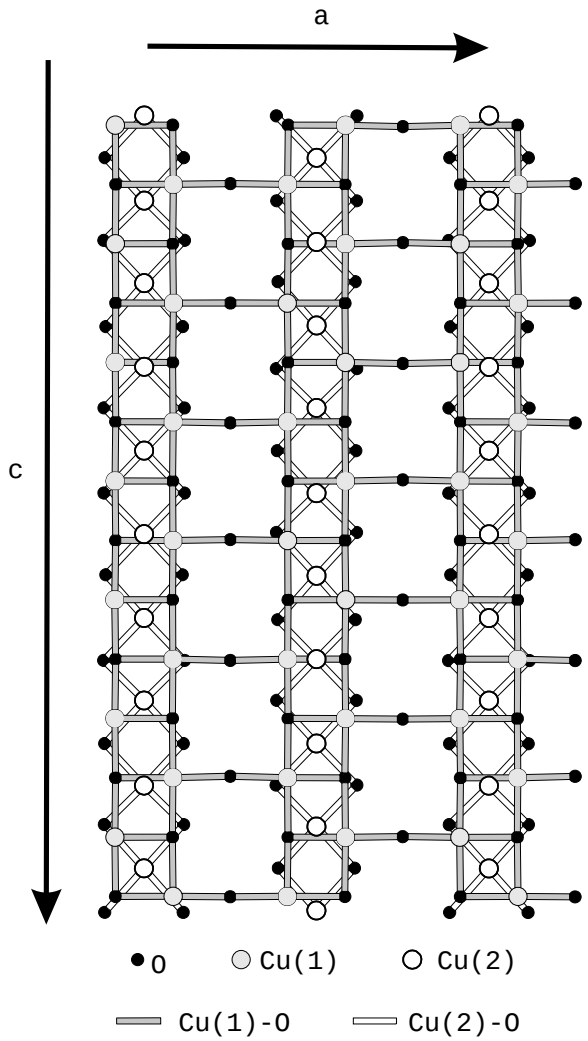

FIG. 2. Relative frameworks of two neighboring $[Cu_2O_3]$ and $[CuO_2]$ layers underlining the ladder structure characteristic. The structural sequence along [001] is drawn within the commensurate approximation; for simplicity, no split sites are considered for the Cu(2) and O(3) atoms.

TABLE 3
Interatomic Distances (Å) Cu–O and *A*–O within the Same Subsystem

	d_{min}	d_{max}	
	First subsystem		
Cu(1)–O(2)	1.872	1.892	$\sigma \approx 0.002$ Å
Cu(1)–O(1)	1.870	1.925	
Cu(1)–O(1^{i})	1.950	1.966	
Cu(1)–O(1^{ii})	1.950	1.966	
A–O(1^{ii})	2.482	2.576	$\sigma \approx 0.002$ Å
A–O(1^{iii})	2.482	2.576	
A–O(2)	2.506	2.644	
A–O(2^{iv})	2.506	2.644	
	Second subsystem		
Cu(2)–O(3^{I})	1.79	2.06	$\sigma \approx 0.004$Å
Cu(2)–O(3^{II})	1.79	2.06	
Cu(2)–O(3)	1.83	2.04	
Cu(2)–O(3^{III})	1.83	2.04	

Note. Symmetry codes: First subsystem: (i) $\frac{1}{2} - x, \frac{1}{2} - y, -\frac{1}{2} + z$; (ii) $\frac{1}{2} - x, \frac{1}{2} - y, \frac{1}{2} + z$; (iii) $\frac{1}{2} + x, y, \frac{1}{2} + z$; (iv) $x, y, 1 + z$. Second subsystem: (I) $X, 1 - Y, \frac{1}{2} - Z$; (II) $\frac{1}{2} - X, Y, \frac{1}{2} - Z$; (III) $X, 1 - Y, \frac{3}{2} - Z$; (IV) $\frac{1}{2} - X, Y, \frac{3}{2} - Z$. The Cu(2)–O(3) distances reported in this table correspond to the most likely configurations (1 or 2, see Fig. 3) for the $Cu(2)O_4$ distorted planar square.

5.2. The Copper Coordination

Inside the first $[A_2Cu_2O_3]$ subsystem, a distorted planar square coordination is observed for Cu(1) atoms in all the crystal. However, in some unit cells defined by the t_1 values close to 0.45 and 0.85, Cu(1) and O(3) atoms are drawn closer up to 2.72 Å; as a result, CuO_5 distorted elongated pyramids are locally formed, suggesting a weak interaction between the copper of the first subsystem and the apical O(3) atom belonging to the second $[CuO_2]$ subsystem (Fig. 1). A similar trend was observed in the composite crystal $Ca_{13.6}Sr_{0.4}Cu_{24+y}O_{41+z}$ ($y = -0.017$, $z = -0.035$) containing a very large amount of Ca(18) and also in the composite crystal $Ca_8La_6Cu_{24}O_{41}$ (12), both of which exhibit commensurate structures with $\gamma = 10/7$. Inside the first $[A_2Cu_2O_3]$ subsystem, two types of Cu–O distances of average values close to 1.89 and 1.96 Å (Table 3) are involved and are consistent, from bond valence calculation (22), with a Cu^{II} valence state. Smooth variations, about 0.02 Å, are observed for three distances while a larger variation of 0.04 Å is found for the Cu(1)–O(1) distance (Table 3). A quite similar coordination is evidenced for Cu(1) in the two crystals I and II studied by Frost-Jensen *et al.* and also in the crystal $Ca_8La_6Cu_{24}O_{41}$ (commensurate case) investigated by Siegrist. These results show that inside the $[Cu_2O_3]$ layers the CuO_4 squares can be considered as rigid bodies in the different spin-ladder cuprates.

Inside the second $[CuO_2]$ subsystem, a distorted planar square coordination is involved for Cu(2) in all the unit cells. The splitting of both Cu(2) and O(3) sites, which most probably is due to disorder phenomena rather than to a lowering of the translational symmetry (no supplementary *HKOM* main reflections were observed), makes the Cu(2) coordination more difficult to explain; fortunately, the splitting is sufficiently marked to foresee the most likely $Cu(2)O_4$ configurations. Examination of the possible Cu(2)–O(3) distances suggests the existence of two main configurations denoted 1 and 2 in Fig. 3, keeping in mind that other configurations are possibly involved. Indeed, among the four possible bonds (only the independent bonds are considered), two of them correspond to unrealistic Cu(2)–O(3) distances, being either too large [2.04 to 2.19 Å] or too small [1.64 to 1.93 Å] in most of the unit cells. The two

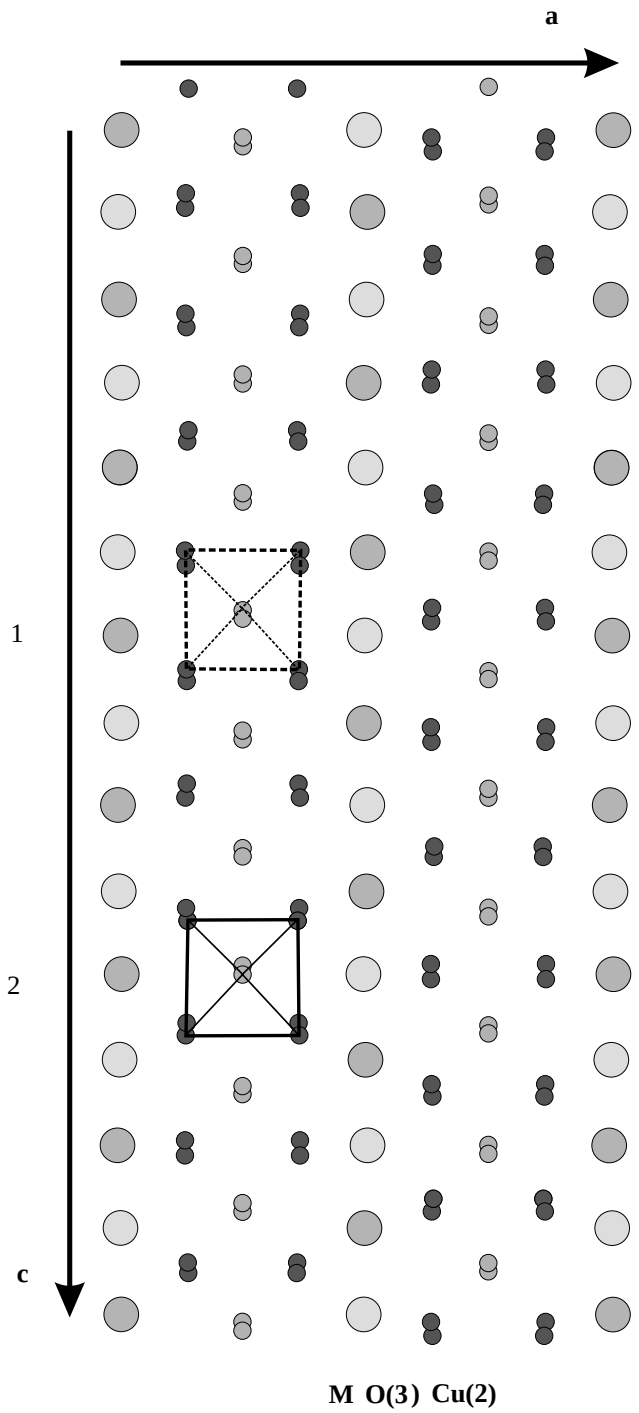

FIG. 3. The two main variants of the CuO_4 square units inside a $[CuO_2]$ layer. The Cu(2) and O(3) split sites are shown within the $y = 0$ layer; the A cations lying in the adjacent layers are shown with dark ($y \approx -1/8$) and gray ($y \approx 1/8$) large circles.

other bonds are characterized (Table 3) by reasonable distances that vary in a significant way versus the t_2 parameter around average values of about 1.92 Å.

Considering single sites for Cu(2) and O(3), the Cu(2)–O(3) distances vary versus t_1 between 1.79 and 2.02 Å. The corresponding variation amplitude is significantly smaller in Frost-Jensen *et al.* crystals I and II, the distances ranging from 1.83 to 1.98 Å and from 1.86 to 1.92 Å, respectively.

5.3. *The A Coordination*

Within the first subsystem, A is linked to four oxygen atoms in all the unit cells. Two main characteristics must be emphasized for the corresponding A–O distances.

(i) The A–O(2)-type distances, where O(2) is bound to two copper atoms, vary in a larger way than the A–O(1)-type distances (see Table 3), where O(1) is linked to three copper atoms. For a comparison the A–O(1) and A–O(2) distances observed in Frost-Jensen's *et al.* crystal I show quite similar variations from 2.52 to 2.60 Å and from 2.54 to 2.62 Å respectively. In crystal II the corresponding distances range from 2.56 to 2.67 Å.

(ii) The four A–O distances are distributed versus the t_1 parameter in an irregular way, suggesting the existence of two types of zones inside the crystal. In the first zone, for t_1 around 0.05 and t_1 around 0.85, the A–O distances exhibit large dispersion; for the maximum one, the distances range from 2.48 to 2.64 Å. In the second zone, for $0.25 < t_1 < 0.65$, the dispersion is reduced, the distances ranging from 2.51 to 2.57 Å. For a comparison, the A–O distances observed in Frost-Jensen's *et al.* crystal I show an uniform dispersion versus t_1 of about 0.08 Å.

The effect described in (ii) can be partly explained from the sinus Fourier term (first harmonic) of the U_3 displacement component (see Table 2) of the A cation, which is significantly larger in our crystal.

Let us now consider the A–O bonds established between A and the O(3) oxygen atom of the $[CuO_2]$ composite part.

Considering single sites for Cu(2) and O(3) the variations of the A–O(3) distances versus t_1 look like those observed in Frost-Jensen's *et al.* crystal I.

However, two characteristics are to be pointed out: first, the minimum values for the A–O(3) distances are slightly different, 2.355 (in our crystal) and 2.375 Å (in Frost-Jensen's *et al.* crystal I). Second, over the full t_1 interval, at least two short A–O(3) distances of about 2.40 Å are observed. For a comparison, these distance types range from 2.355 to 2.420 Å and from 2.375 to 2.470 Å in our crystal and in Frost-Jensen's *et al.* crystal I, respectively. As expected, in crystal II ($A = Bi_{0.04}Sr_{0.96}$) the A–O(3) minimum distance becomes longer, 2.46 Å. The splitting of the previous sites gives rise to some difficulty in studying the A–O(3) bonding scheme. However significant results can be derived. The minimum values of the A–O(3) distances are smaller within this split model, about 2.30 Å. To obtain sound hypotheses concerning the A–O(3) bonding scheme, an A–O(3) distance

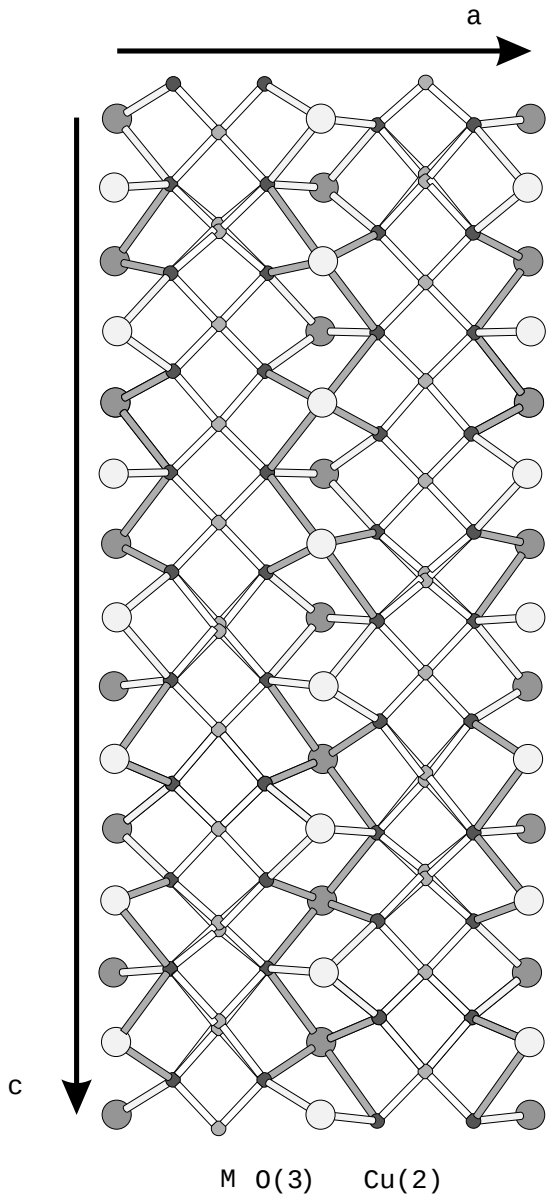

FIG. 4. The two types of A–O(3) environment. A possible Cu(2)–O(3) and A–O(3) bonding scheme is suggested (commensurate approximation) starting from the split model (Fig. 3).

calculation was performed within the commensurate approximation $7c_1 \approx 10c_2$, including all the A cations ($y = -1/8$ and $y \approx 1/8$ layers) close to the $[CuO_2]$ layer ($y = 0$). A possible sequence of the A–O(3) bonds along the [001] misfit direction is depicted in Fig. 4. Note that this hypothesis leads, on average, to CuO_4 configurations with realistic Cu–O distances since the configurations 1 and 2 (Fig. 3) mainly occur; the two other possible configurations, the "compressed" and the "dilated" ones, would require for Cu(2) an average position, rather than one of the two split positions, to obtain realistic Cu(2)–O(3) bond distances.

Despite some ambiguity concerning this bonding scheme along [001], a significant trend can be evidenced: the A cations show indeed two types of O(3) environment (Fig. 4), including either three or four oxygen atoms (a limit distance of about 3.0 Å is assumed for the A–O bond). Otherwise, from refinement results, Ca and Sr atoms are distributed at random on the A sites; as a result, these two types of cation would display seven- and eightfold coordination in this composite crystal. To give a more accurate description of this coordination, the A–O distances found in the first five unit cells, running along [001], are listed in Table 4.

A calculation, as a function of t_1, of the A valence according to the bond valence formalism (22), taking into account the splitting of the O(3) sites also appears consistent with an hazardous occupation of the A sites by Ca and Sr atoms. Considering indeed an average value $\langle R \rangle$ for the R parameter, characteristic of the A–O bond, with $\langle R \rangle = \alpha R_{Ca} + \beta R_{Sr}$, α and β denoting the Ca and Sr percentages, an average valence close to 2 is obtained for A, with minimal and maximal values of 1.93 and 2.11.

Finally, the improvement of the agreement R factors, observed by introducing split sites for Cu(2) and O(3), would lead to assuming the existence of a positional disorder within the $[CuO_2]$ chains; running along a given chain, four different configurations would occur for the CuO_4 squares, most probably with only a local order, in such a way that the configurations 1 and 2 are the main ones.

This structural scheme seems to be consistent, to a certain extent, with the model suggested by Wu *et al.* (16), who explain the disorder in the $[CuO_2]$ subsystem from a phase shift of the modulation wave; this phase shift would occur with some chance stage running along [001].

TABLE 4
The A coordination; A–O distances in Angstrom

n_3					
0	**1**	**2**	**3**	**4**	
2.49	2.51	2.48	2.52	2.52	$\sigma \approx 0.002$ Å
2.56	2.51	2.57	2.54	2.55	
2.61	2.55	2.60	2.56	2.57	
2.64	2.55	2.64	2.56	2.58	
2.30	2.35	**2.29**	**2.30**	2.30	$\sigma \approx 0.004$ Å
2.33	**2.35**	**2.33**	2.32	**2.30**	
2.39	2.49	2.41	2.44	**2.43**	
2.39	**2.50**	2.41	**2.55**	**2.50**	
2.57	**2.78**	2.50	**2.55**	2.52	
2.60	2.81	**2.52**	2.62	2.54	
2.87		2.94			

Note. The n_3 integers specify, running along [001], the unit cells of the first sublattice. Inside each cell, the first four A–O distances involve the O(1)- and O(2)-type oxygen atoms while the others are related to the O(3) oxygen atoms of the second sublattice. The distances with bold-faced type correspond to one of the two O(3) split sites.

In conclusion, this 4D structural study of a calcium-rich spin-ladder composite crystal $[A_2Cu_2O_3]_{7+\delta}[CuO_2]_{10}$ with $A = Sr_{0.43}Ca_{0.55}Bi_{0.03}$ evidences without ambiguity disorder phenomena inside the $[CuO_2]$ subsystem, involving a splitting of both Cu and O sites. The latter can be interpreted by the existence of two different configurations of CuO_4 groups inside the $[CuO_2]$ layers. The structure of this phase differs also from that determined by Frost-Jensen *et al*., which contains less calcium, by a larger modulation amplitude and by the existence of weak Cu–O interactions (2.72 Å) between the Cu atoms of one $[Cu_2O_3]$ layer and the oxygen atoms of the next CuO_2 layer.

ACKNOWLEDGMENTS

During the course of this study, Lydia Leonyuk passed away on September 2000, fighting against cancer. We will miss her enthusiasm, her superb expertise, and her friendship. A. Maignan is gratefully acknowledged for performing the superconductivity tests. We are also indebted to Mrs J. Chardon and Mrs R. Aguinet for their technical assistance.

REFERENCES

1. B. Raveau, C. Michel, M. Hervieu, and D. Groult, "Crystal Chemistry of High-T_C Superconducting Copper Oxides." Springer-Verlag, Berlin, 1991.
2. A. Yamamoto, M. Onoda, E. Takayama-Muromachi, F. Izumi, T. Ishigaki, and H. Asano, *Phys. Rev. B* **42,** 4228–4239 (1990).
3. V. Petricek, Y. Gao, P. Lee, and P. Coppens, *Phys. Rev. B* **42,** 387–392 (1990).
4. A. A. Levin, Yu. I. Smolin, and Yu. F. Shepelev, *J. Phys. Condens. Matter* **6,** 3539–3551 (1994).
5. D. Grebille, H. Leligny, A. Ruyter, P. Labbé, and B. Raveau, *Acta Crystallogr. Sect. B* **52,** 628–642 (1996).
6. H. Leligny, S. Durcok, P. Labbé, M. Ledésert, and B. Raveau, *Acta Crystallogr. Sect. B* **48,** 407–418 (1992).
7. P. A. Miles, S. J. Kennedy, G. J. Mc Intyre, G. D. Gu, G. J. Russell, and N. Koshizuka, *Physica C* **294,** 275–288 (1998).
8. C. L. Teske and H. K. Müller-Buschbaum, *Z. Anorg. Allg. Chem.* **370,** 134 (1969).
9. T. M. Rice, S. Gopalan, and M. Siegrist, *Europhys. Lett.* **23,** 445 (1993).
10. M. Takano, Z. Hiroi, and M. Azuma, *ICR Annu. Rep.* **2,** 20 (1995).
11. L. Leonyuk, V. Rybakov, E. Sokolova, V. Maltsev, L. Shvanskaya, G. J. Babonas, R. Szymczak, H. Szymczak, and M. Baran, *Z. Kristallogr* **213,** 406–410 (1998).
12. T. Siegrist, L. F. Schnemeyer, S. A. Sunshine, J. V. Wascak, and R. S. Roth, *Mater. Res. Bull.* **23,** 1429 (1988).
13. E. M. MacCarron, M. A. Subramanian, J. C. Calabrese, and R. L. Harlow, *Mater. Res. Bull.* **23,** 1355 (1988).
14. A. Frost-Jensen, F. K. Larsen, B. B. Iversen, V. Petricek, T. Schultz, and Y. Gao, *Acta Crystallogr. Sect. B* **53,** 113–124 (1997).
15. A. Frost-Jensen, V. Petricek, F. K. Larsen, and E. McCarron, *Acta Crystallogr. Sect. B.* **53,** 125–134 (1997).
16. X. J. Wu, E. Takayama-Muromachi, S. Suehara, and S. Horiuchi, *Acta Crystallogr. Sect. A* **47,** 727–735 (1991).
17. V. Petricek and M. Dusek, Crystallographic computing system JANA 98, Tech. Rept. Institute of Physics, Academy of Sciences of the Czech Republik, Prague, 1998.
18. T. Ohta, F. Izumi, M. Onoda, M. Isobe, E. Takayama-Muromachi, and W. Hewat, *Phys. Soc. Jpn.* **66,** 3107–3114 (1997).
19. A. Yamamoto, *Acta Crystallogr. Sect. A* **48,** 476–483 (1992).
20. K. Trueblood, H. Burgi, H. Burzlaff, J. Dunitz, C. Gramaccioli, H. Schulz, U. Shmueli, and S. Abrahams, *Acta Crystallogr. Sect. A* **52,** 770–781 (1996).
21. S. Pachot, Thesis, Joseph Fourier Grenoble I University, 1999.
22. N. Brese and M. O'Keefee, *Acta Crystallogr. Sect. B* **47,** 192–197 (1991).